Research Article

Thokozani Xaba*

Green synthesis of ZnS nanoparticles and fabrication of ZnS–chitosan nanocomposites for the removal of Cr(VI) ion from wastewater

https://doi.org/10.1515/gps-2021-0026
received June 10, 2020; accepted November 24, 2020

Abstract: A modified homogeneous precipitation method has been used to synthesize ZnS nanoparticles. Starch and polyvinyl alcohol (PVA) were utilized as capping molecules, and later, the ZnS–PVA-capped nanoparticles were then incorporated with chitosan to form ZnS–chitosan nanocomposites for the removal of Cr(VI) ion from wastewater. The optical measurements of the synthesized ZnS nanoparticles showed the band gap which was blue-shifted when compared with the bulk ZnS material. The crystalline structures were determined by X-ray diffraction, and the crystalline sizes were estimated from the Scherer formula. XRD spectra confirmed the formation of hexagonal phase for the uncapped ZnS nanoparticles with an average crystalline size of 3.71 nm whereas the starch- and PVA-capped ZnS nanoparticles showed the formation of cubic phase structures with crystalline sizes of 3.26 and 2.88 nm. The TEM image showed spherical particles with regular morphologies and significantly narrow size distributions. The calculated average particle diameters were in good agreement with the estimated XRD result. The removal of Cr(VI) ion from wastewater was studied through the adsorption process. The effect of pH, dosage, and contact time was investigated. More than 95% of the metal ion recovery was achieved through using ZnS–chitosan nanocomposites.

Keywords: zinc sulfide nanoparticles, chitosan, nanocomposites, Cr(VI) ions, adsorption

1 Introduction

The extreme discharge of heavy metals into the environment due to industrialization and urbanization has created difficult challenges worldwide. The existence of heavy metal ions in the water systems is a major concern due to their toxicity and non-biodegradability which can cause problems to the environment [1]. The high concentrations of these heavy metals in the effluents may trigger hindrance with biological treatment processes at the sewage treatment systems [2]. Among these heavy metals, chromium is graded as one of the top sixteen toxic pollutants that have harmful effects on human well-being [3]. A high concentration of chromium can cause a bad effect on human kidneys and livers [4]. A high quantity of chromium can also cause cancer in the intestinal and lungs [5].

Heavy metals can be treated from wastewater through reverse osmosis, precipitation, ultra-filtration membrane filtration, adsorption, co-precipitation, adsorption, solvent extraction, and membrane process [6]. Among these techniques, the adsorption process has been proven to be a highly effective method that has been used lately for the removal of heavy metals from waste streams. It has been proven to be cost-effective, long-lasting, renewal adsorbent, and an easy method to operate when compared with the other techniques [7].

In recent years, various types of coagulants have shown potential applications in wastewater and water treatment. Chitosan, which is a non-toxic linear high molecular weight cationic polymer, has been used lately as a coagulant in water treatment since it has an ability to interact with the bacterial surface. It has been endorsed as a potentially eco-friendly coagulant and flocculant due to its natural biological characteristics and biodegradability [8]. The combination of nanomaterials with chitosan to form the polymer nanocomposite can coactively improve the antimicrobial effect of the polymer material. This unification usually improves the surface charge of

* **Corresponding author: Thokozani Xaba,** Department of Chemistry, Vaal University of Technology, P/Bag X021, Vanderbijlpark, South Africa, e-mail: thokozanix@vut.ac.za

the composite and also increases multiply sites for bonding with metal centers during wastewater treatment.

Nano-sized materials have attracted a great deal of interest over the years in scientific societies due to their exceptional and interesting physical, chemical, and biological properties [9]. Semiconducting materials, especially the metal chalcogenides, have been studied due to their wide bandgap and their application in solar cells, optoelectronics, optical sensor devices, photoluminescence, etc. [10]. Among metal chalcogenides, zinc sulfide (ZnS) has been studied and revealed significant properties for unique diverse applications in electroluminescence [11], lasers [12], light-emitting diodes (LEDs) [13], and bio-devices [14]. ZnS is an important II–VI chalcogenide with a wide direct band gap of 3.77 eV for the wurtzite structure [15] as well as 3.72 eV for the zinc blende structure [16]. ZnS is also regarded as a low-cost and non-toxic material with high resistance to photochemical degradation [17]. Several methods have been reported for the synthesis of zinc sulfide nanoparticles that include hydrothermal technique [18], microwave irradiation [19], solvothermal [20], and wet chemical or co-precipitation methods [10]. During the synthesis of nanomaterials, it is important to use chemical processes that eliminate the use of toxic and harmful substances. Designing and utilizing green chemistry approaches for the synthesis of nanomaterials can help to protect the environment. The homogeneous precipitation method is regarded as an alternative technique that eliminates the usage of non-hazardous substances [21,22].

Past research findings have proven that the combination of nanomaterials with the polymeric substance such as chitosan to form the polymer nanocomposite can improve and increase the surface charge of the polymer and eventually multiply the number of bonding sites that can allow the metal ions to be attracted on the surface of the nanocomposites during the adsorption process [23]. In our previous study, thiosemicarbazone ligand was successfully used in the synthesis of ZnS nanoparticles and the preparation of ZnS–polydadmac nanocomposites. The influence of the concentration of green capping agents as stabilizers was studied [24]. Tiwari et al. [25] reported the synthesis and optical properties of polymer-based ZnS nanocomposites. PVA, starch, and hydroxypropylmethyl cellulose were used due to their non-toxicity, water solubility, and biocompatibility. The effect of hydroxyl-functionalized polymers on ZnS and their optical properties was studied. The results showed that hydroxyl-functionalized polymers were much effective at nucleating and stabilizing ZnS nanoparticles when compared with the other polymers. A review based on the removal of chromium from industrial effluents using nanotechnology was reported by Mitra et al. [26] while Owalude and Tella [27] reported the removal of hexavalent chromium from aqueous solutions by adsorption on modified groundnut hull. The modified groundnut shell was found to be the better adsorbent of Cr(VI) ions when compared with the unmodified groundnut shell.

Most of the technologies that have been used in water treatment together with their starting materials are generally expensive, complicated, and time-consuming. To the best of my knowledge, there is no study that has been reported in the past for the removal of Cr(VI) from wastewater using the ZnS–chitosan as an adsorbent that was prepared from a simple, cost-effective, and easy environmental method such as the homogeneous precipitation method. Thus, in the present study, the preparation of ZnS nanoparticles capped with starch and PVA via the greener route and the preparation of ZnS–chitosan nanocomposites is reported. The prepared polymer nanocomposites and chitosan were used as adsorbents to remove Cr(VI) ions from wastewater through a batch experiment. The percentage removal was also determined. Factors such as the changes in pH of solutions, dosage, and contact time were investigated. The optical properties were characterized with UV–Vis and PL. The structural and morphological properties have been studied using XRD and TEM whereas the flame atomic absorption spectrophotometry (AAS) was utilized to measure the concentrations of the solutions.

2 Materials and methods

2.1 Materials

Thiourea, 1-methyl-2 pyrrolidone, zinc acetate dihydrate, starch, PVA, ammonium hydroxide, chitosan, chromium salt, methanol, and acetone were reagents from Sigma-Aldrich and were all used without further purification.

2.2 Experimental

2.2.1 Synthesis of the zinc sulfide nanoparticles

The (*Z*)-2-(1-methyl-pyrrolidin-2-ylidene) thiourea ligand was prepared according to the method described previously [24,28]. ZnS nanoparticles were synthesized by mixing zinc acetate (5 mmol) in warm 50% methanol

(20 mL) with (20 mL) warm 50% methanolic solution of the ligand (10 mmol) in a 100 mL two necked flask. The warm mixture was refluxed inside the water bath at 70°C for an hour to produce a white solution. Exactly, 0.5% starch or PVA solution was added into the white solution to stabilize the nanoparticles. The pH of the solution was adjusted to pH = 11 with ammonia hydroxide solution and further stirred for an hour. The synthesized ZnS nanoparticles were separated from the solution using the centrifuge technique, washed three times with acetone, and dried in an open-air.

2.2.2 Preparation of ZnS–chitosan nanocomposites

The synthesized ZnS–PVA-capped nanoparticles (~3 mg) were dispersed in 10 mL of distilled water. The filtered nanoparticle solution was then transferred into a small beaker with 50 mL of 0.5% chitosan solution that was previously prepared from dilute acetic acid. The beaker with the mixture was then sealed with a foil and placed inside an ultra-sonic bath for 4 h to ensure complete unification. The prepared ZnS nanocomposite solution was then used in water treatment.

2.2.3 Batch adsorption experiments

A stock solution of heavy metal (1,000 ppm) was prepared by dissolving 2.83 g of Cr(VI) salt in 1 L of distilled water. The desired concentrations ranging from 20 to 100 ppm were obtained by the dilution method. For each experiment of adsorption, 20 mL of the ion metal solution was shaken at 250 rpm in a plastic bottle. The pH of the solution was adjusted to the desired value by adding 0.1 M NaOH or 1.0 M HCl. Batch adsorption studies were carried out using the thermostat shaker at room temperature at a speed rate of 250 rpm.

2.3 Characterization

UV-1800 Shimadzu spectrophotometer and Gilden fluorescence spectrometer were used to measure the optical properties of ZnS nanoparticles. The nanoparticles were dissolved in distilled water, and the solution was placed in a quartz cuvette with a path length of 1 cm. XRD patterns of the samples were obtained from a Phillips X'Pert chemistry research diffractometer using secondary monochromated Cu Kα radiation (λ = 1.54060 Å) at 40 kV/30 mA. Measurements were taken using a glancing angle of incidence detector at an angle of 2θ values over 10 to 80 degrees in steps of 0.0167 with a scan speed of 0.0452. Transmission electron microscopy (TEM) was performed using a Tecnai F30 FEG TEM instrument at an accelerating voltage of 300 kV. TEM samples were prepared by placing 1 or 2 drops of ZnS nanoparticles dissolved in water/acetone mixture on lacey carbon copper grids to obtain TEM images. AAS analysis was collected from the AA-7000 Shimadzu model coated GFA-7000 graphite furnace atomizer.

3 Results and discussion

3.1 Zinc sulfide nanoparticles

The substituted thiourea ligand was prepared from the reaction of 1-methyl-2-pyrrolidone with thiourea. The ligand was then used to synthesize zinc sulfide nanoparticles through the homogeneous precipitation method as represented in Scheme 1. The incorporation of ZnS nanoparticles into chitosan to form ZnS–chitosan nanocomposites has been explored. The nanocomposites were then used in water treatment to remove Cr(VI) ions from wastewater.

3.1.1 Optical properties

The optical absorption spectra of ZnS nanoparticles have been carried out using UV–Vis spectroscopy. Figure 1a shows the optical absorption profile with the band edges at 299, 275, and 256 nm for the (i) uncapped, (ii) starch-, and (iii) PVA-capped ZnS nanoparticles. It was observed that as the capping molecule is introduced into the nanoparticles, the spectra were blue-shifted which is an indication of the decrease in sizes of the particles. To determine the band gap of the ZnS nanoparticles, a plot of absorbance square versus energy (eV) was done. The band gap energies were estimated by extrapolating the steepest part of the curve. The results are represented in Figure 1b. The band gap of the ZnS nanoparticles was observed at 4.09, 4.35, and 4.34 eV, which were blue-shifted when compared with the bulk ZnS material [29,30].

Photoluminescence is an instrumental technique that was used to study the luminescence properties of the ZnS nanomaterials and is presented in Figure 1c. The emission spectra show the maximum peaks at 311 nm (3.99 eV) for

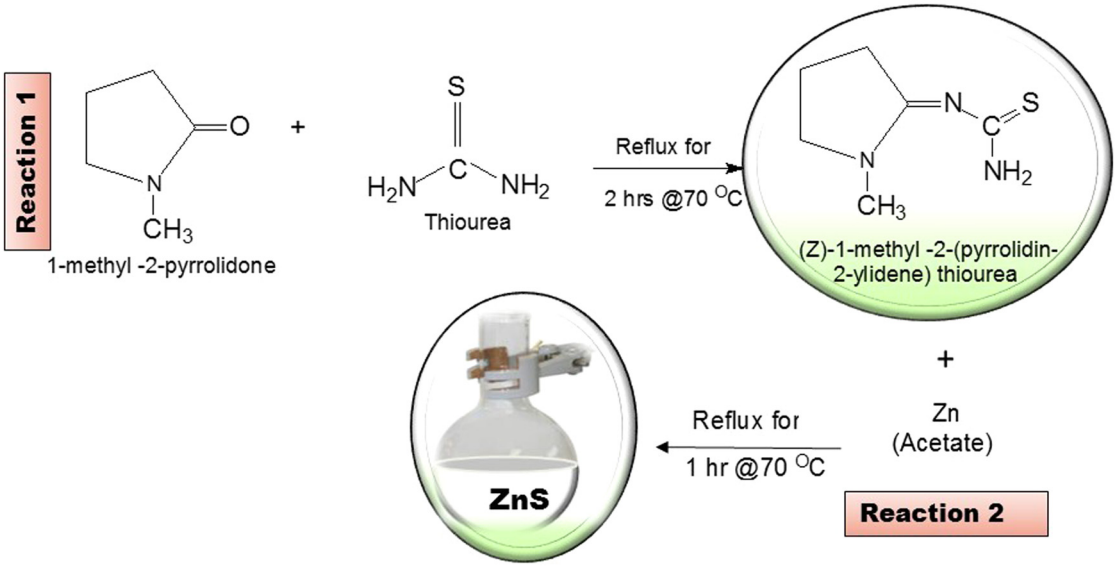

Scheme 1: Preparation of the (*Z*)-2-(1-methyl-pyrrolidin-2-ylidene) thiourea ligand and the synthesis of ZnS nanoparticles.

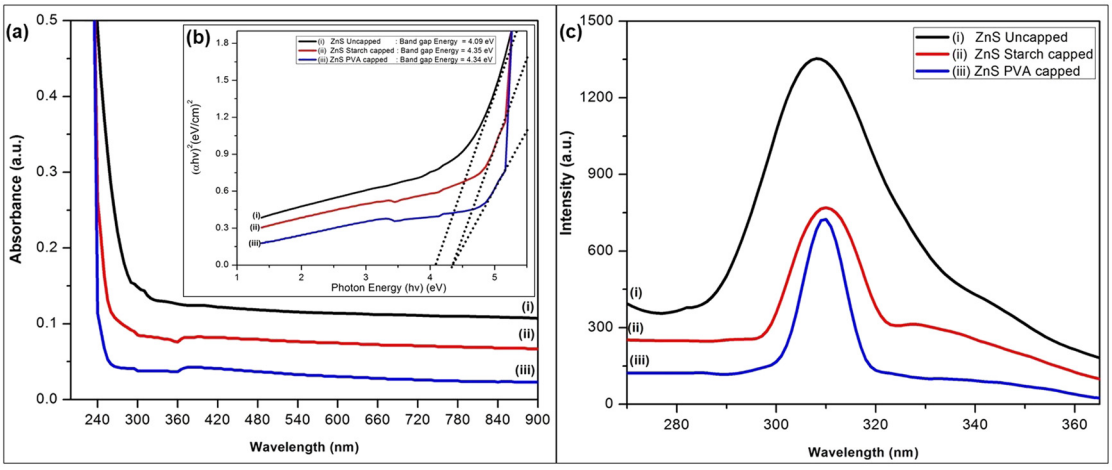

Figure 1: Absorption (a), Tauc plot (b), and emission spectra (c) of ZnS uncapped (i), starch- (ii), and PVA- (iii) capped nanoparticles.

the uncapped ZnS nanoparticles (Figure 1c(i)) while both capped ZnS nanoparticles reveal maxima peaks at 309 nm (4.01 eV) in Figure 1c(ii,iii).

3.1.2 Structural properties

Figure 2a shows the FTIR spectra of the uncapped, starch-, and PVA-capped ZnS nanoparticles. The spectral measurements were carried out in the range between 500 and 4,000 cm^{-1} at room temperature. The FTIR spectra of all ZnS nanoparticles show the same absorption band at about 3,366 and 3,012 cm^{-1} for the uncapped ZnS nanoparticles, which correspond to the O–H vibrations of the capping agents and O–H stretching of the water molecules [28,31,32]. The remaining peaks of the uncapped ZnS nanoparticles in Figure 2a(i) were shifted toward the lower frequency when compared with the absorption peaks of the capped ZnS nanoparticles. The absorption bands between 660–674 cm^{-1} and 598–612 cm^{-1} from the FTIR spectra of the uncapped, starch-, and PVA-capped ZnS nanoparticles are attributed to the zinc sulfide bond [33].

XRD patterns of the synthesized ZnS nanoparticles are shown in Figure 2b. The diffraction peaks of the uncapped nanoparticles in Figure 2b(i) show the 2θ values located at 26.72°, 28.42°, 30.85°, 38.38°, 48.33°, 51.41°, 53.53°, 55.00°, 57.56°, 61.12°, 70.45°, and 75.05° which correspond to (100), (002), (101), (102), (110), (103), (200),

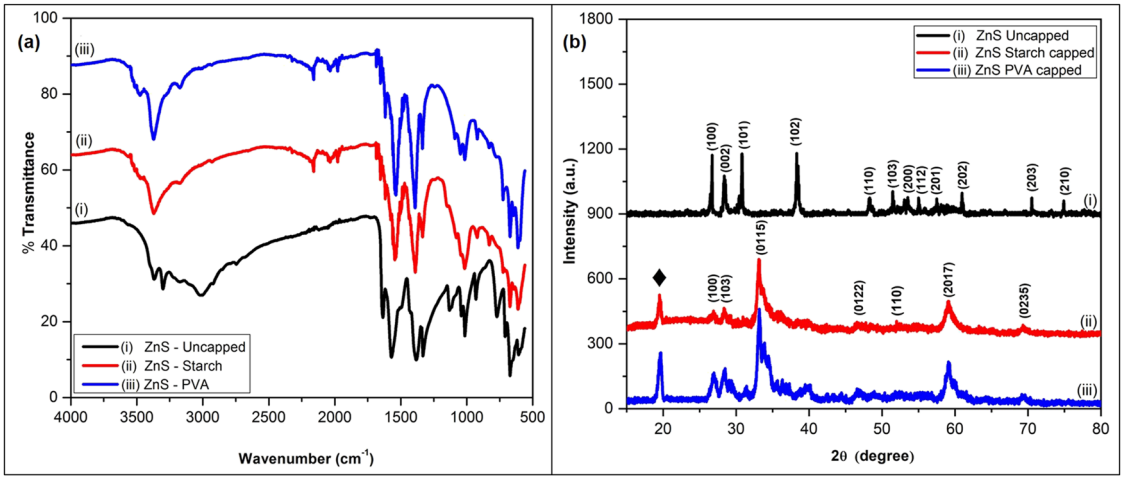

Figure 2: FTIR spectra (a) and X-ray diffraction patterns (b) of ZnS uncapped (i), starch- (ii), and PVA- (iii) capped nanoparticles.

(112), (201), (202), (203), and (210), respectively. These planes are indexed to a hexagonal phase which matches with JCPDS card No: 79-2204 whereas Figure 2b(ii,iii) of the starch- and PVA-capped ZnS nanoparticles show the 2θ values located at 26.90°, 28.41°, 33.25°, 36.86°, 46.73°, 59.18°, and 69.35° which correspond to (100), (103), (0115), (0122), (110), (2017), and (0235), respectively, which can be indexed to cubic phase with the JCPDS card number: 01-072-9259. These results are in consistent with the reported results [24]. The diffraction peaks at 19.67° and 19.76° correspond to the starch and PVA, respectively

The crystalline sizes of the synthesized ZnS nanoparticles were calculated using the Debye–Scherrer formula in Eq. 1 [34]:

$$D = \frac{0.9(\lambda)}{\beta \cos \theta}, \tag{1}$$

where D is the particle size in nm, 0.9 is a Scherrer's constant, λ is the wavelength of X-rays, θ is the Bragg diffraction angle, and β is the full-width at half-maximum (FWHM) of the diffraction peak corresponding to the maximum peaks. The average particle sizes of the nanoparticles were found to be 3.71, 3.26, and 2.88 nm for the uncapped, starch-capped, and PVA-capped ZnS nanoparticles, respectively.

Figure 3 shows TEM nanographs of the synthesized ZnS nanocrystallines. The TEM images for all the nanoparticles showed spherical-shaped particles and uniform sizes with average diameters of 3.71 ± 0.653, 3.49 ± 0.383, and 2.71 ± 0.423 nm for the uncapped and capped ZnS nanoparticles. These results were in good agreement with the sizes determined from XRD analysis by Scherrer's equation. The large particle size value of the uncapped ZnS nanoparticles may be due to the particle aggregation which might be caused by potential environmental factors since the nanoparticles were not protected by capping molecules [35].

3.2 Adsorption studies

Parameters such as pH, adsorbent dosage, and contact time can play an important role in the removal of Cr(VI) from wastewater. The initial concentration of the Cr(VI) solution of 100 ppm (20 mL) was used throughout and the Whatman filter paper No. 42 was utilized to filter the solutions. Flame atomic absorption spectrophotometry (AAs) was used to analyze the adsorbed amount of Cr(VI) by the nanocomposites from wastewater and the percentage removal of Cr(VI) was calculated using Eq. 2 [36]:

$$\% \text{ Removal} = \frac{C_0 - C_1}{C_0} \times 100\% \tag{2}$$

where C_0 (ppm) is the initial metal ion concentration and C_1 (ppm) is the final metal ion concentration in the solution.

3.2.1 Effect of pH

The study based on the effect of pH in adsorption is a very essential factor since it regulates the adsorbent's surface charges. Previous reports confirm that the binding sites of the metal cation and adsorbent become protonated at low pH values. It had been reported that repulsion occurs

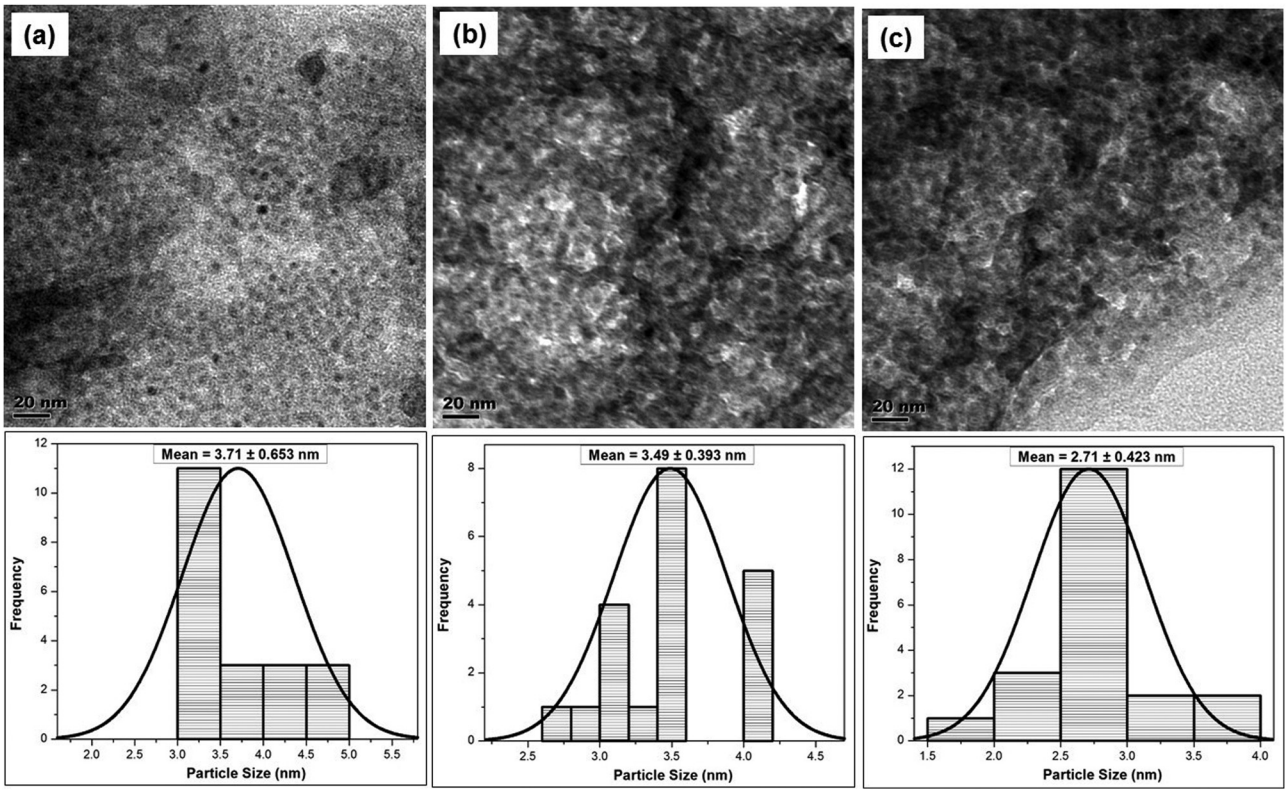

Figure 3: TEM image of ZnS uncapped (a), starch- (b), and PVA- (c) capped nanoparticles.

between the metal cation and the adsorbent at higher pH. The binding spots begin to deprotonate and generate different functional groups available for binding [37].

The effect of pH of the solution was varied using the initial concentration of 100 ppm for Cr(VI) solution. The percentage removal of the Cr(VI) ions at different pH values is represented in Figure 4. The results show that at the pH between 4 and 8, the percentage removal of Cr(VI) is low for both the ZnS–chitosan and chitosan. As the pH is increased from 8 to 11, the percentage removal of the metal cation was also increased to a maximum percentage of 95.99% for ZnS–chitosan and a maximum percentage of 62.96% for pure chitosan. The optimum pH = 9 for both adsorbents was observed.

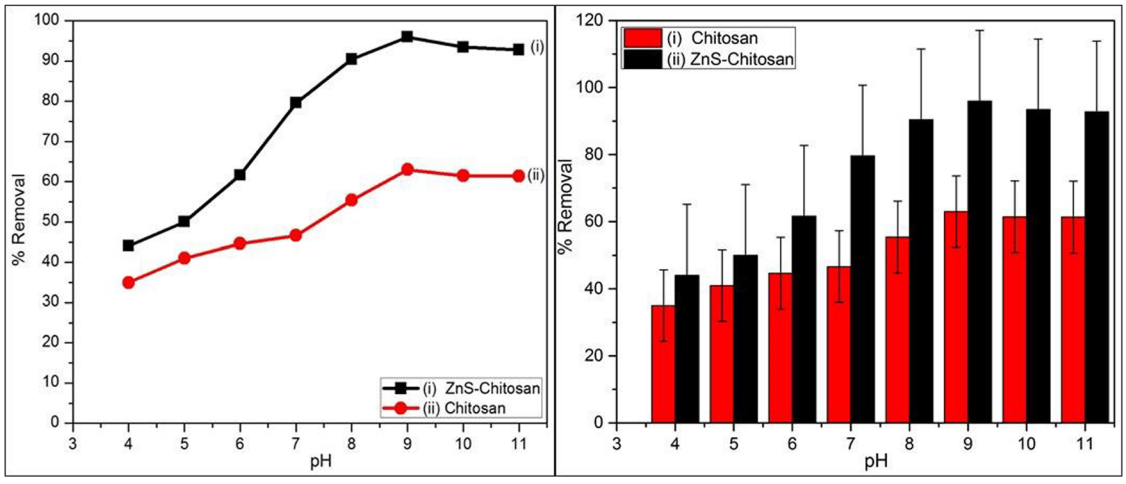

Figure 4: Effect of pH on adsorption of Cr(VI) ion using chitosan (i) and ZnS–chitosan nanocomposites (ii) as absorbents.

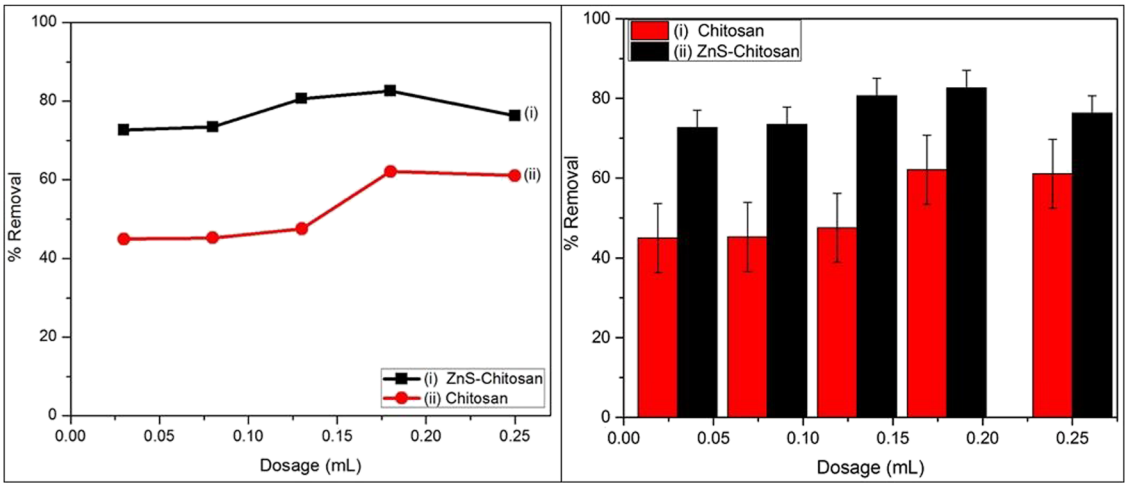

Figure 5: Effect of dosage on adsorption of Cr(VI) ion using chitosan (i) and ZnS–chitosan nanocomposites (ii) as absorbents.

3.2.2 Effect of adsorbent dosages

Effect of adsorbent dosage in Figure 5 was carried out at pH = 9 as it showed a greater percentage removal of metal ions. It was noted that the percentage removal was increasing to 59.79% and 80.91% when the amount of chitosan or ZnS–chitosan nanocomposites raised from 0.03 to 0.25 mL. About 0.18 mL was found to be the maximum adsorbent dosage.

3.2.3 Effect of contact time

The effect of contact time is the most important parameter for economical wastewater treatment systems [23]. In six different containers, 20 mL of the Cr(VI) ion solution was transferred. Each sample was treated with 0.18 mL nanocomposites and shaken with thermo shaker in different time intervals of 15, 30, 60, 120, 240, and 300 min, respectively. The results in Figure 6 show that Cr(VI) ion removal is increasing with an increase in contact time. The results project the removal capacity of the metal ion to 65.60% and 94.79% when chitosan and ZnS–chitosan nanocomposites are used as absorbents. The equilibrium was reached at 240 min by both absorbents.

3.2.4 Mechanism of Cr(VI) ion removal

Generally, the adsorption of heavy metals depends on the surface area and pore structure of the adsorbent [38]. The surface area of the nanocomposites consists of amino and

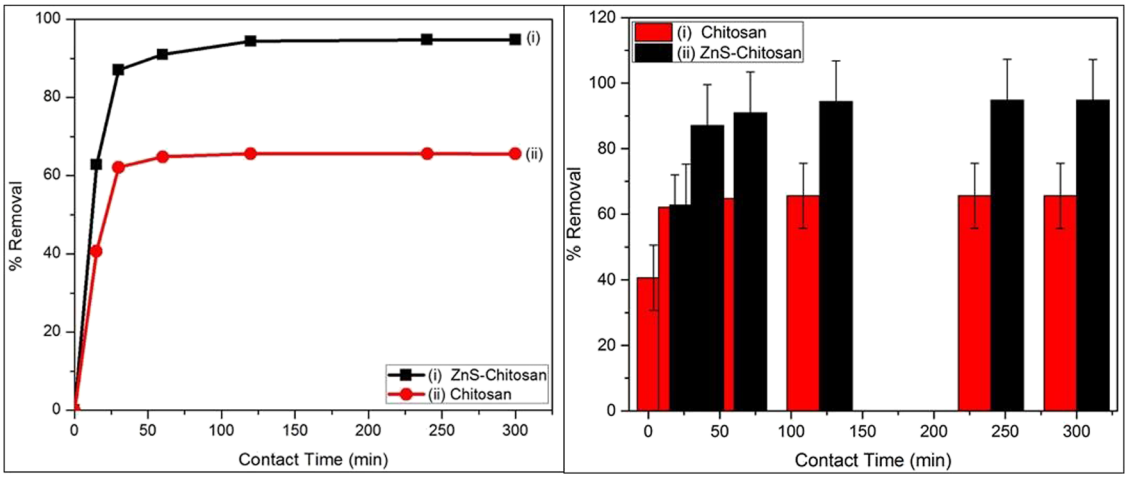

Figure 6: Effect of contact time on adsorption of Cr(VI) ion using chitosan (i) and ZnS–chitosan nanocomposites (ii) as absorbents.

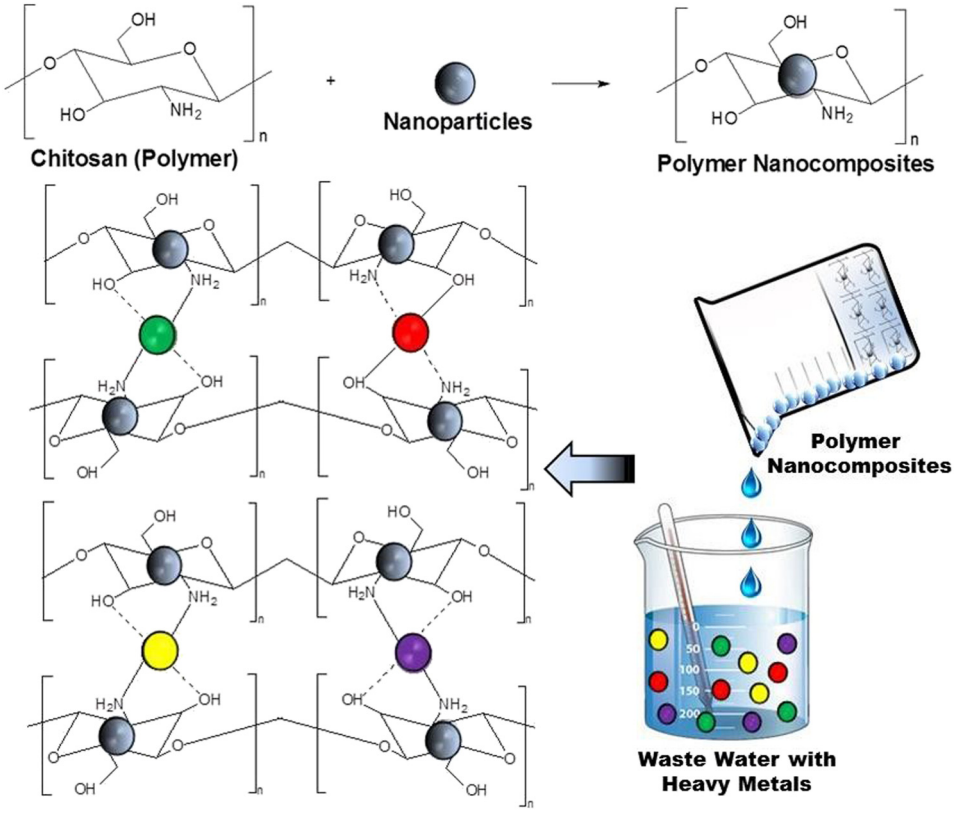

Scheme 2: The formation of nanocomposites and the adsorption of heavy metal on chitosan-based nanocomposites.

hydroxyl groups that are designed to bind with the Cr(VI) ions. Adsorption of Cr(VI) ion onto chitosan and nanocomposites depends on the amino and hydroxyl groups [39]. The lone pair that is available in the nitrogen and oxygen atoms are existing to the empty atomic orbitals of the Cr(VI) ion, which forms coordination complexes on the surface of the material [40] as represented by Scheme 2 below by Xaba et al. [23].

4 Conclusion

The ZnS nanoparticles were synthesized through the homogeneous precipitation method. The optical properties of the capped nanoparticles showed a blue shift in wavelength when compared with the uncapped ZnS nanoparticles. The XRD studies show a cubic phase for the capped nanoparticles whereas the uncapped nanoparticles projected hexagonal phase crystal structures. TEM images for the synthesized ZnS nanoparticles showed spherical-shaped particles. These results corroborated well with the XRD results. The highest percentage removal of Cr(VI) ion from wastewater was achieved when ZnS–chitosan nanocomposite was used as an adsorbent. The obtained data may be useful in designing and fabricating an economical wastewaters treatment that possesses a high concentration of chromium(VI) ions.

Acknowledgment: The author would like to acknowledge the Vaal University of Technology for the support.

Funding information: The study was funded by the National Research Foundation (TTK13071722088: "Thuthuka Grant Holder").

Author contributions: Thokozani Xaba confirms sole responsibility for the following: study conception and design, data collection, analysis and interpretation of results, and manuscript preparation.

Conflict of interest: The author states no conflict of interest.

Data availability statement: The datasets generated or analyzed during the current study are available from the corresponding author on reasonable request.

References

[1] Gupta VK, Gupta M, Sharma S. Process development for the removal of lead and chromium from aqueous solution using red mud–an aluminum industry waste. Water Res. 2001;35:1125–34.

[2] Tahir SS, Rauf N. Removal of Fe(II) from the wastewater of a galvanized pipe manufacturing industry by adsorption onto bentonite clay. J Environ Manag. 2004;73(4):285–92.

[3] Gardea-Torresdey JL, Tiemann KJ, Armendariz V, Bess-Oberto L, Chianelli RR, Rios J, et al. Characterization of Cr(VI) binding and reduction to Cr(III) by the agricultural by products of Avena monida (Oat) biomass. J Hazard Mater. 2000;80(1–3):175–88.

[4] Mungasavalli DP, Viraraghavan T, Jin YC. Biosorption of chromium from aqueous solution by pretreated Aspergillus niger: batch and column studies. Colloids Surf A Physicochem Eng Asp. 2007;301(1–3):214–23.

[5] Ofudje EA, Awotula AO, Oladipo GO, Williams OD. Detoxification of chromium(VI) ions in aqueous solution via adsorption by raw and activated carbon prepared from sugarcane waste. Covenant J Phys Life Sci. 2014;2(2):110–22.

[6] Li Q, Zhai J, Zhang W, Wang M, Zhou J. Kinetic studies of adsorption of Pb(II), Cr(III) and Cu(II) from aqueous solution by sawdust and modified peanut husk. J Hazard Mater. 2007;141(1):163–7.

[7] Beh CL, Chuah TG, Nourouzi MN, Choong TSY. Removal of heavy metals from steel making waste water by using electric arc furnace slag. E-J Chem. 2012;9(4):2557–64.

[8] Renault F, Sancey B, Badot P-M, Crini G. Chitosan for coagulation/flocculation processes – an eco-friendly approach. Eur Polym J. 2009;45(5):1337–48.

[9] Azam A, Ahmed AS, Oves M, Khan MS, Memic A. Size-dependent antimicrobial properties of CuO nanoparticles against Gram-positive and -negative bacterial strains. Int J Nanomed. 2012;7:3527–35.

[10] Palve AM. Deposition of zinc sulfide thin films from Zinc(II) thiosemicarbazones as single molecular precursors using aerosol assisted chemical vapour deposition technique. Front Mater. 2019;6:46.

[11] Tang W, Cameron DC. Electroluminescent zinc sulphide devices produced by sol-gel processing. Thin Solid Films. 1996;280(1–2):221–6.

[12] Biswas S, Ghoshal T, Kar S, Chakrabarti S, Chaudhuri S. ZnS nanowire arrays: synthesis, optical and field emission properties. Cry Growth Des. 2008;8(7):2171–6.

[13] Luo Y, Duan G, Ye M, Zhang Y, Li G. Poly(ethylene glycol)-mediated synthesis of hollow ZnS microspheres. J Phys Chem C. 2008;112(7):2349–52.

[14] Lin KB, Su YH. Photoluminescence of Cu:ZnS, Ag:ZnS, and Au:ZnS nanoparticles applied in Bio-LED. Appl Phys B. 2013;113(3):351–9.

[15] Ong HC, Chang RPH. Optical constants of wurtzite ZnS thin films determined by spectroscopic ellipsometry. Appl Phys Lett. 2001;79(22):3612–314.

[16] Tran TK, Park W, Tong W, Kyi MM, Wagner V, Summers CJ. Photoluminescence properties of ZnS epilayers. J Appl Phys. 1997;81(6):2803–9.

[17] Dilpazir S, Siddiq M, Iqbal A. Synthesis of zinc sulphide nanostructures by Co-precipitation: effects of doping on electro-optical properties. Kenkyu J Nanotechnol Nanosci. 2015;1:34–9.

[18] Hoa TTQ, Vu LV, Canh TD, Long NN. Preparation of ZnS nanoparticles by hydrothermal method. J Phys. 2009;187:012081–7.

[19] Zhao Y, Hong JM, Zhu JJ. Microwave-assisted self-assembled ZnS nanoballs. J Cryst Growth. 2004;270(3–4):438–45.

[20] Park J, Joo J, Kwon SG, Jang Y, Hyeon T. Synthesis of monodisperse spherical nanocrystals. Angew Chem Int Ed. 2007;46(25):4630–60.

[21] Díaz-Cruz C, Alonso Nuñez G, Espinoza-Gómez H, Flores-López LZ. Effect of molecular weight of PEG or PVA as reducing-stabilizing agent in the green synthesis of silver-nanoparticles. Eur Polym J. 2016;83:265–77.

[22] Xaba T, Moloto MJ, Moloto N. The effect of water-soluble capping molecules in the "Green" synthesis of CdS nanoparticles using the (Z)-2-(pyrrolidin-2-ylidene)thiourea ligand. Mater Lett. 2015;146:91–5.

[23] Xaba T, Moloto MJ, Nchoe O, Nate Z, Moloto N. Synthesis of silver sulfide nanoparticles through homogeneous precipitation route and the preparation of the Ag_2S-chitosan nanocomposites for the removal of iron(II) ion from wastewater. Chalcogenide Lett. 2017;14(8):337–46.

[24] Xaba T, Moloto MJ, Al-Shakban M, Malik AM, Moloto N, O'Brien P. The influence of concentration of green capping agents and ammonium solution as an "activator and stabilizer" in the synthesis of ZnS nanoparticles for the preparation of the polymer nanocomposites. Green Process Synth. 2017;6(2):173–82.

[25] Tiwari A, Khan SA, Kher RS, Dhoble SJ, Chandel ALS. Synthesis characterization and optical properties of polymer-based ZnS nanocomposites. Luminescence. 2016;31(2):428–32.

[26] Mitra S, Sarkar A, Sen S. Removal of chromium from industrial effluents using nanotechnology: a review. Nanotechnol Environ Eng. 2017;2(1):1–11.

[27] Owalude SO, Tella AC. Removal of hexavalent chromium from aqueous solutions by adsorption on modified groundnut hull. Beni-Suef Univ J Basic Appl Sci. 2016;5(4):377–88.

[28] Xaba T, Magagula J, Nchoe OB. Green Synthesis of Cu_2S nanoparticles from (Z)-1-methyl-2-(pyrrolidin-2-ylidene) thiourea ligand for the preparation of Cu_2S-Chitosan nanocomposites for the removal of Cr(VI) ion from wastewater. Mater Lett. 2018;229:331–5.

[29] Murugadoss G, Rajamannan B, Ramasamy V. Synthesis, characterization and optical properties of water-soluble ZnS:Mn^{2+} nanoparticles. J Lumin. 2010;130(11):2032–9.

[30] Lakshmi PVB, Raj KS, Ramachandran K. Synthesis and characterization of nano ZnS doped with Mn. Cryst Res Technol. 2009;44(2):153–8.

[31] Vetrone F, Boyer JC, Capobianco JA. Yttrium oxide nanocrystals: luminescent properties and applications. Am Sci Publ Ed. 2004;10:725–65.

[32] Divya Rao M, Pennathur G. Facile bio-inspired synthesis of zinc sulfide nanoparticles using chlamydomonas reinhardtii cell free extract: optimization, characterization and optical properties. Green Process Synth. 2016;5(4):379–88.

[33] Rema Devi BS, Raveendran R, Vaidyan AV. Synthesis and characterization of Mn^{2+}-doped ZnS nanoparticles. Pramana. 2007;68(4):679–87.
[34] Panda SK, Antonakos A, Liarokapis E, Bhattacharya S, Chaudhuri S. Optical properties of nanocrystalline SnS_2 thin films. Mater Res Bull. 2007;42(3):576–83.
[35] Korshed P, Li L, Ngo DT, Wang T. Effect of storage conditions on the long-term stability of bactericidal effects for laser generated silver nanoparticles. Nanomaterials (Basel). 2018;8(4):218.
[36] Milonjic SK, Boskovic MR, Ceranic TS. Adsoprtion of uranium (VI) and zirconium(IV) from acid solutions on silica gel. Sep Sci Technol. 1992;27:1643–53.
[37] Hadi AG. Removal of Fe(II) and Zn(II) ions from aqueous solutions by synthesized chitosan. Int J Chemtech Res. 2016;9(4):343–9.
[38] Kuchta B, Firlej L, Maurin G. Modeling of adsorption in nanopores. J Mol Model. 2005;11(4–5):293–300.
[39] Yu K, Ho J, McCandlish E, Buckley B, Patel R, Li Z, et al. Copper ion adsorption by chitosan nanoparticles and alginate microparticles for water purification applications. Colloids Surf A Physicochem Eng Asp. 2013;425:31–41.
[40] Futalan CM, Kan C-C, Dalida ML, Pascua C, Wan M-W. Fixed-bed column studies on the removal of copper using chitosan immobilized on bentonite. Carbohydr Polym. 2011;83(2):697–704.